



Analysis of Cu – water nanofluid flow with different particle shapes over an isothermal moving plate

Santosh Chaudhary*

Department of Mathematics, Malaviya National Institute of Technology, Jaipur 302 017, India

E-mail: d11.santosh@yahoo.com

Received 19 August 2021; accepted 18 April 2022

Contribution of Cu (copper) nanoparticle shapes in base fluid – water on nanofluid flow over a moving plate has been scrutinized. Five classic models of nanoparticle shapes (sphere, cube, triangular pyramid, cylinder, lamina) have been taken into account. Employing similarity transformation, basic boundary layer controlling equations have been reduced to a set of nonlinear ordinary differential equations. Solutions have been attained numerically for them by executing the MATLAB's boundary layer problem solver (bvp4c). Outcomes have, then, been applied to compare the influence of pertinent parameters on velocity and temperature graphically, while, the impact on shear stress and heat flux have been compared in tables. Moving parameter, sphericity and shape of Cu nanoparticles have been the significant controlling parameters.

Keywords: Moving plate, Nanofluid, Cu nanoparticle shapes

Nanofluid is a well-versed term for the uniform suspension of ultrafine nanoparticles in conventional base fluids at minimum possible concentrations. The size of solid nanoparticles usually range in diameter less than 100 nm and their concentration is typically small (<10% by volume). Nanoparticles used in nanofluid are frequently made up of metals (Cu , Ag , Au , Ni), metal oxides (Ag_2O_3 , CuO , TiO_2 , SiO_2 , ZnO , MgO), metal nitride (AlN), metal carbides (SiC) and carbon nanotubes. Some popular base fluids used are water, oils, toluene, ethylene glycol and polymerized or plasticised solutions. The suspension remains stable because of relatively similar size of nanoparticles and molecules of the base fluid. Around the mid-90s, nanofluids were discovered by Choi¹ and from 2000 onwards, it started gaining huge attention from the scientific community because of its wide-ranging engineering and industrial applications. Conventional coolants such as ethylene glycol, water and oils have lower thermal conductivity which directed scientists to develop novel coolants with enhanced thermal properties. Insertion of nano-sized particles in these fluids is among possible techniques to augment the conductivity of standard coolants. Xuan and Li² divulged their analysis of features of heat transfer of nanofluids. Chein and Chuang³ experimentally studied the performance of Microchannel Heat Sink using nanofluids. Evidently, the dispersion of nano-sized particles in a base fluid may cause an increase or

decrease of heat transfer coefficient of a nano-fluid with respect to the base fluid. The viscosity of the nanofluid escalates rapidly at higher nanoparticle volume fraction, suppressing the heat transfer augmentation in the nanofluid. It is therefore, crucial to carefully opt the suitable nanoparticle volume fraction to achieve heat transfer enhancement. The increment in thermal conductivity of the base-fluid due to the presence of nanoparticles has been observed in the range of 15-40%. The nano-material conductivity is susceptible to plenty of factors like type of nanoparticles; shape, size, concentration and stability of dispersed nanoparticles and which base-fluid is utilized. Akbarinia and Laur⁴ explored the impacts of different sized nanoparticles on laminar nanofluid flow and then published the investigation. Enhancement of heat transfer due to nanofluids is numerically analyzed by various researchers including but not limited to Yang and Lai⁵, and Rana and Bhargava⁶.

Nanofluids have attracted the attention of researchers from diverse fields of science and engineering technology due to their enormous industrial applications. Some well-known analytical investigations regarding nanofluids are done by Hamad and Ferdows⁷, Mital⁸, Pal and Mandal⁹, and Vanaki and Mohammed¹⁰. Eventually, heat transfer characteristics of Cu – water nanofluid and Al_2O_3 – water nanofluid are reported by Hayat *et al.*¹¹ and

Reddy and Chamkha¹², respectively. Some of the innumerable applications of nanofluids are in the manufacturing process of heat changer equipment and electronic cooling system radiators, pharmaceutical processes, microelectronics, nuclear reactor coolant, hybrid-powered engines and space technology. Nanofluids also have various applications in medical field such as safer surgery by cooling and cancer therapy. A plethora of researches like¹³⁻¹⁶ have been published ranging from fundamentals of production and determination of thermal properties and analysis of physical mechanisms related to nanofluids. Recently, Chaudhary and Kanika¹⁷ worked on the investigations related to nanofluid flow based on carbon nanotubes and Mishra *et al.*¹⁸ described MHD flow of nanofluids in presence of a heat source. Lately, the work on bioconvective nanofluid flow with viscous dissipation in porous medium has been conducted by Alluguvelli *et al.*¹⁹.

Sakiadis²⁰ was the first one who pointed out that boundary layer on a flat surface and a moving solid surface is different. Thenceforth, the analysis of boundary layer flows driven by moving plate have been published by many researchers like Fang²¹, Mahmoud and Mahmoud²², Bachok *et al.*²³, Mukhopadhyay *et al.*²⁴ and manymore. Chaudhary and Kumar²⁵ gave an interesting investigation of boundary layer flow over a flat plate. However, there is equivalent or in fact more practical importance of studies of the flow and heat transfer properties caused by continuously moving surface. Some widely used applications of this concept, in engineering and technical processes, are in polymer industry, spinning of fibres, extrusion of plastic sheets, lamination and melt spinning processes. Keeping this fact in mind, Chaudhary and Choudhary²⁶ considered boundary layer flow over a flat surface moving in parallel free stream. The problems of nanofluid flow over permeable moving plate have occupied the attention of a few researchers, one of such, is Anuar *et al.*²⁷. Recently, Zainal *et al.*²⁸ studied the flow of nanofluid over permeable moving surface.

Malvandi *et al.*²⁹ worked to analyse the thermodynamics of fluid flow over moving plate. The present study aims to extend the above research work using nanofluids and explore the consequence of different shapes of nanoparticles on fluid behaviour. The current research work presents new and original study and is not published elsewhere to the best of author's knowledge.

Experimental Section

Modeling

Let us consider a two-dimensional, time-independent boundary layer flow of a nanofluid over a moving surface which motions in the same and also the reverse direction to free stream with variable velocities. The fluids taken into account are viscous incompressible Cu – water nanofluids with various nanoparticle shapes. The physical model with detailed geometries has been illustrated in Fig. 1. The x – axis is assumed along the flat plate and y – axis is perpendicular to it and flow is confined to $y > 0$. The velocity of the moving plate is maintained at U_w and the free stream velocity U_∞ is taken as uniform ($U_\infty > 0$). In addition, $U_w > 0$ implies that the flat surface is moving in the positive x – direction, while $U_w < 0$ defines the movement of the surface in the negative x – direction. The wall temperature is assumed to be constant and equal to T_w while the temperature of the nanofluid far away from the flat surface is T_∞ ($T_w > T_\infty$). Under these assumptions, the governing basic boundary layer equations for this problem are expressed as

$$\frac{\partial u}{\partial x} + \frac{\partial v}{\partial y} = 0 \quad \dots (1)$$

$$\rho_{nf} \left(u \frac{\partial u}{\partial x} + v \frac{\partial v}{\partial y} \right) = \mu_{nf} \frac{\partial^2 u}{\partial y^2} \quad \dots (2)$$

$$(\rho C_p)_{nf} \left(u \frac{\partial T}{\partial x} + v \frac{\partial T}{\partial y} \right) = \kappa_{nf} \frac{\partial^2 T}{\partial y^2} \quad \dots (3)$$

Subject to the boundary conditions for the flow field

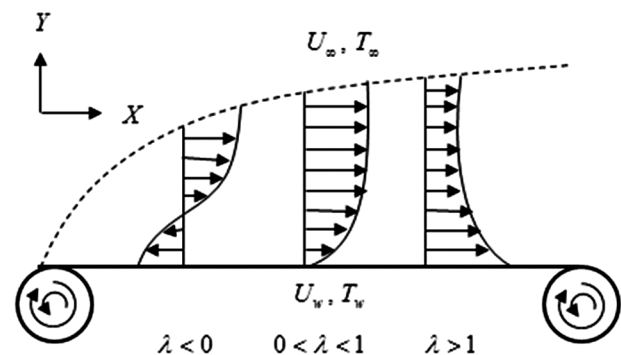


Fig. 1 — Flow geometry.

$$\begin{aligned} v = 0, u = U_w, T = T_w \quad \text{at } y = 0 \\ u \rightarrow U_\infty, T \rightarrow T_\infty \quad \text{as } y \rightarrow \infty \end{aligned} \quad \dots (4)$$

In the above equations, the subscript *nf* represents the characteristics of nanofluid, *u* and *v* are the flow velocity components in *x*- and *y*- axes, respectively, $\rho \left(= \frac{\mu}{\nu} \right)$ is the density, μ is the coefficient of viscosity, ν is the kinematic viscosity, C_p is the specific heat at constant pressure, *T* is the temperature of nanofluid and κ is the thermal conductivity. Moreover, thermo-physical properties of base fluid water and the *Cu* nanoparticles are presented in Table 1 as mentioned by Oztop and Abu-Nada³⁰. From Mohammad and Kandasamy³¹, the thermo-physical models for the physical quantities - density, dynamic viscosity, heat capacity and thermal conductivity of nano fluid are given in Table 2.

In Table 2, subscripts *f* and *s* denote base fluid and solid nanoparticles, respectively, ϕ is the solid volume fraction, $m \left(= \frac{3}{\Phi} \right)$ is the empirical shape factor, Φ is the sphericity of the particles. The value of Φ is unity for sphere and <1 for an irregular shaped particle. Values of sphericity of *Cu* nanoparticles (*Lin et al.*³²) along with corresponding shapes – sphere, cube, triangular pyramid, cylinder, and lamina are illustrated in Table 3, as considered in the present investigation.

Similarity Variables

Introducing dimensionless variables as given by Malvandi *et al.*²⁹

Table 1 — Thermo-physical properties of base fluid and nanoparticles.

Properties	Water	<i>Cu</i>
$\rho(Kg/m^3)$	997.1	8933
$C_p(J/Kg K)$	4179	385
$\kappa(W/mK)$	0.613	400

Table 2— Thermo-physical models of nanofluids.


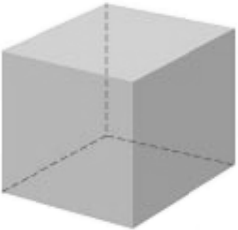
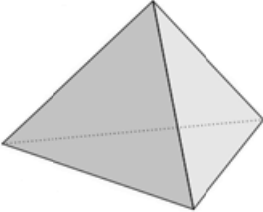


Physical Properties	Nanofluid
Density (ρ)	$\rho_{nf} = (1 - \phi)\rho_f + \phi\rho_s$
Dynamic viscosity (μ)	$\mu_{nf} = \frac{\mu_f}{(1 - \phi)^{5/2}}$
Heat capacity (ρC_p)	$(\rho C_p)_{nf} = (1 - \phi)(\rho C_p)_f + \phi(\rho C_p)_s$
Thermal conductivity (κ)	$\kappa_{nf} = \frac{(m - 1)\kappa_f + \kappa_s - (m - 1)\phi(\kappa_f - \kappa_s)}{(m - 1)\kappa_f + \kappa_s + \phi(\kappa_f - \kappa_s)} \kappa_f$

$$\psi = (2\nu_f U_\infty x)^{1/2} f(\eta), \quad \eta = \left(\frac{U_\infty}{2\nu_f x} \right)^{1/2} y, \quad T = (T_w - T_\infty)\theta(\eta) + T_\infty \quad \dots (5)$$

Here ψ is the stream function that satisfies the continuity equation (1) automatically with $u = \frac{\partial \psi}{\partial y}$ and $v = -\frac{\partial \psi}{\partial x}$, *f* is the non-dimensional stream function, η is the similarity variable and θ is the non-dimensional temperature.

Using the similarity transformations equation (5) along with the expression in Table 2, in equations (2)

Table 3 — Nanoparticle shapes and their sphericity.

Model	Shape	Φ
	Sphere	1.0000
	Cube	0.8060
	Triangular Pyramid	0.7387
	Cylinder	0.4710
	Lamina	0.1857

to (4), the following nonlinear ordinary differential equations are obtained

$$f''' + (1-\phi)^{5/2} \left(1 - \phi + \phi \frac{\rho_s}{\rho_f} \right) f f'' = 0 \quad \dots (6)$$

$$\frac{\kappa_{nf}}{\kappa_f} \theta'' + \left[1 - \phi + \phi \frac{(\rho C_p)_s}{(\rho C_p)_f} \right] \text{Pr} f \theta' = 0 \quad \dots (7)$$

with conditions

$$\begin{aligned} f = 0, f' = \lambda, \theta = 1 \quad \text{at } \eta = 0 \\ f' \rightarrow 1, \theta \rightarrow 0 \quad \text{as } \eta \rightarrow \infty \end{aligned} \quad \dots (8)$$

where primes denote the function derivative with respect to η . $\text{Pr} \left(= \frac{\nu \rho C_p}{\kappa} \right)$ is the Prandtl number and $\lambda \left(= \frac{U_w}{U_\infty} \right)$ is the velocity ratio parameter.

Declaration of Curiosity

Quantities of practical interest are skin friction coefficient (C_f) and local Nusselt number (Nu_x), expressed as

$$C_f = \frac{\tau_w}{\rho_f U_\infty^2}, \quad Nu_x = \frac{x q_w}{\kappa_f (T_w - T_\infty)} \quad \dots (9)$$

In the above equation, $\tau_w = \mu_{nf} \left(\frac{\partial u}{\partial y} \right)_{y=0}$ is the surface shear stress and $q_w = -\kappa_{nf} \left(\frac{\partial T}{\partial y} \right)_{y=0}$ is the surface heat flux.

Using dimensionless variables equation (5), the equation (9) is obtained as follows

$$\left(\frac{\text{Re}_x}{2} \right)^{1/2} C_f = \frac{1}{(1-\phi)^{5/2}} f''(0), \quad \left(\frac{2}{\text{Re}_x} \right)^{1/2} Nu_x = -\frac{\kappa_{nf}}{\kappa_f} \theta'(0) \quad \dots (10)$$

there $\text{Re}_x = \frac{U_\infty x}{\nu_f}$ is the local Reynolds number.

Solution methodology and validation

To obtain the computational solution of similarity equations (6) and (7) under the appropriate boundary conditions [Equation (8)], MATLAB's built-in function `bvp4c` is utilized for selected values of embedded parameters as the moving parameter (λ),

the nanoparticle volume fraction (ϕ) and various shapes of the *Cu* nanoparticles while keeping the Prandtl number fixed for water ($\text{Pr} = 6.2$). For the computational procedure, the finite value of boundary conditions as $\eta \rightarrow \infty = 4$ is employed. The step size is taken as $\Delta \eta = 0.001$ to achieve a convergence criterion of 10^{-7} asymptotically, for all cases considered. The acquired numerical results give an understanding about the flow structure concerning velocity $f'(\eta)$ and temperature $\theta(\eta)$ profiles and numerical values of skin friction coefficient (C_f) and local Nusselt number (Nu_x).

In order to validate the credibility of the numerical results, they are compared with the data in the previously published literature for the surface shear stress $f''(0)$ in the absence of λ and ϕ (Presented in Table 4). It is, hence, verified that the results obtained are accurate and the solution methodology used is appropriate for the present problem.

Results and Discussion

To explain the theoretical concept of the discussed model, the effect of the controlling parameters on fluid flow $f'(\eta)$ and temperature $\theta(\eta)$ is graphically represented in Figures 2-6, while the variations in the surface shear stress $f''(0)$ and the surface heat flux $\theta'(0)$ are tabulated in Table 5. The controlling parameters considered in this problem are moving parameter λ , nanoparticle volume fraction ϕ and various shapes of the *Cu* nanoparticles. The analysis of the behavior of particular flow model is done by observing one parameter at a time, while keeping other relevant parameters constant.

Figures 2 and 3 elaborate the influence of λ on $f'(\eta)$ and $\theta(\eta)$, respectively. Based on these, it is noted that momentum boundary layer increases with a rise in λ , while the reverse effect is observed on the

Table 4 — Comparison of $f''(0)$ at $\lambda = \phi = 0$.

Researchers	$f''(0)$
Yacob et al. ³³	0.46960
Present outputs $\eta \rightarrow \infty = 4$	0.47118
$\eta \rightarrow \infty = 5$	0.46968
$\eta \rightarrow \infty = 6$	0.46960
$\eta \rightarrow \infty = 7$	0.46960
$\eta \rightarrow \infty = 8$	0.46960

thermal boundary layer. As depicted in figure 1, the nanofluid flow is analyzed for $\lambda < 0, 0 < \lambda < 1$ and $\lambda > 1$. It is also significant that Fig. 2 is in good agreement with the schematic boundary layers shown

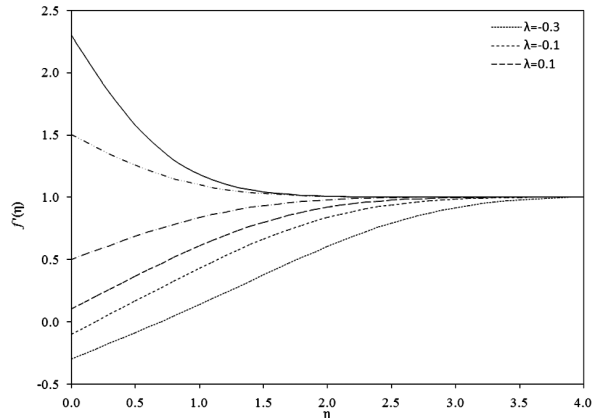


Fig. 2 — Dimensionless velocity profiles for different values of λ with $\phi = 0.08$.

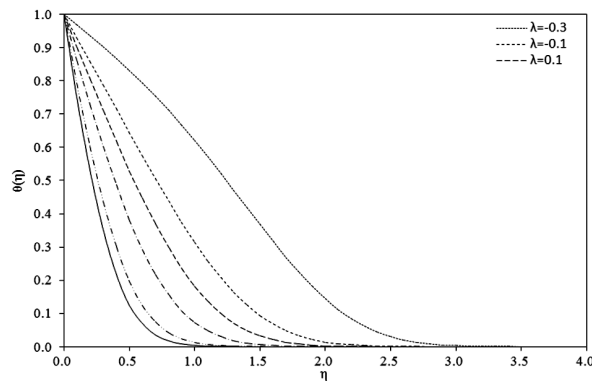


Fig. 3 — Dimensionless temperature profiles for different values of λ with $\phi = 0.08$ and $m = 3$.

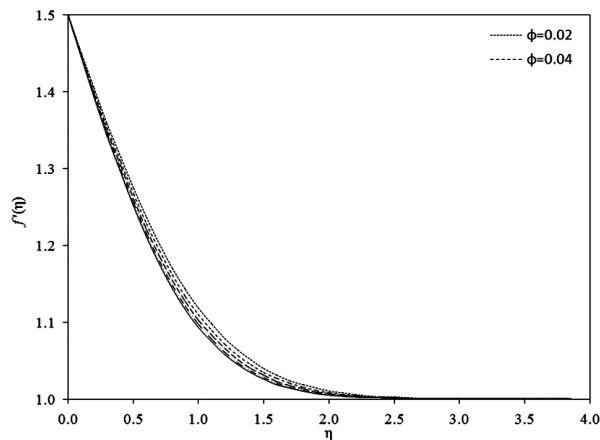


Fig. 4 — Dimensionless velocity profiles for different values of ϕ with $\lambda = 1.5$.

in Fig. 1. Velocity ratio parameter λ is greater than zero when the plate moves in the direction of the free stream and $0 < \lambda < 1$ indicates that its motion is slower than velocity of the nanofluid. The boundary layer is observed to become thinner as λ approaches unity. However, increase in boundary layer thickness with rising value of λ is observed after the flat plate's velocity becomes more than that of free stream ($\lambda > 1$) owing to the pulling force of plate exerted on fluid which reverses the frictional force. It is remarkably illustrated in Fig. 3 that as the values of moving parameter elevate, the temperature drops on account of higher heat transfer due to the surge in momentum transfer close to the flat plate.

Influence of nanoparticle concentration on velocities and temperature distribution are plotted in Figs 4 and 5, respectively. Enhancement in solid volume fraction ϕ leads to dampening of velocity profile as a consequence of aggravation in the resistance of nanofluid flow. Insertion of more

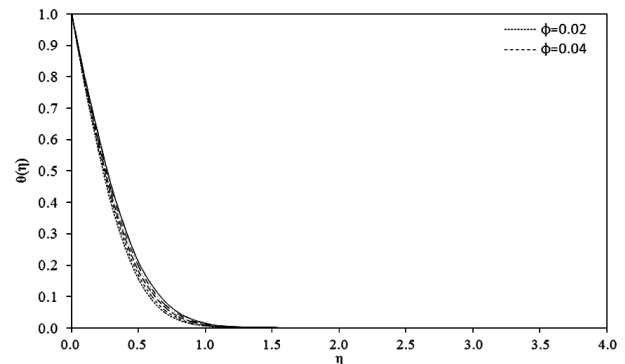


Fig. 5 — Dimensionless temperature profiles for different values of ϕ with $\lambda = 1.5$ and $m = 3$.

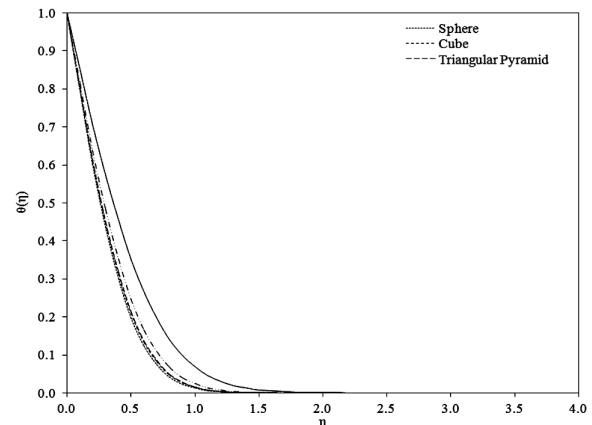


Fig. 6 — Dimensionless temperature profiles for different nano particle shapes with $\lambda = 1.5$ and $\phi = 0.08$.

Table 5 — Results of $f''(0)$ and $\theta'(0)$ for certain values of physical parameters with $Pr = 6.2$.

λ	ϕ	Solids shape	$-f''(0)$	$-\theta'(0)$
-0.3	0.08	Sphere	-0.41869	0.322559
-0.1			-0.53200	0.704170
0.1			-0.53329	0.970043
0.5			-0.37899	1.371407
1.5			0.52764	2.077050
2.3			1.61270	2.507314
1.5	0.02	Cube	0.48054	2.288810
	0.04		0.49943	2.214646
	0.06		0.51500	2.144173
	0.10		0.53773	2.012973
	0.08		0.52764	2.025940
			Triangular Pyramid	2.003207
			Cylinder	1.866472
		Lamina	1.495811	

nanoparticles boosts the thermal conductivity resulting in the increment of the temperature when nanoparticle volume fraction is increased.

The temperature variation $\theta(\eta)$, portrayed in Fig. 6, are attributable to the different nanoparticle shapes with the same base fluid. When the value of sphericity (Φ) declines, or empirical shape factor (m) increases, it is perceived from the graph that temperature escalates as: sphere < cube < triangular pyramid < cylinder < lamina.

Range of values in Table 5 represent that $f''(0)$ dwindles with greater nanoparticle volume fraction ϕ and moving parameter for $\lambda > 0$. At $\lambda = 0$ (stationary plate), the local skin friction coefficient is maximum. Thereafter, for $\lambda < 0$, both λ and $f''(0)$ increase correspondingly. The significance of positive sign of surface shear stress is the drag force exerted by nanofluid on moving plate, whereas negative sign suggests the opposite.

The numerical set of values in table 5 also reveal that the local Nusselt number increases with enhancement of ϕ which connotes the amplification of thermal conductivity as a result of increased nanoparticle dispersion. Whereas, the heat transfer rate $\theta'(0)$ is observed to become smaller with rising moving parameter λ and sphericity Φ by virtue of diverse shapes of nanoparticles utilized. The values of heat flux $\theta'(0)$ are found to be always negative for every considered value of the parameters. Focusing on physical concept, it implies that the heat flow is occurring from surface to nanofluid.

Conclusion

An overview of the investigation of flow properties of Cu – water nanofluid over an isothermal moving flat plate is given in this section. Conversion of the governing partial differential equations into non-dimensional ordinary differential equations has been done utilizing similarity transformation. Numerical results were obtained by solving them further via MATLAB and are summarized as follows

- (i) Velocity boundary layer thickness and shear stress ($\lambda < 0$) was found to be elevated while shear stress ($\lambda > 0$), thermal boundary layer thickness and heat flux rate dropped with increasing moving parameter.
- (ii) Step-up of the solid volume fraction leads to step-down of the velocity and local skin friction coefficient and escalation of temperature and local Nusselt number.
- (iii) Lamina shaped nanoparticle were found to have a superior effect on enhancing values of nanofluid temperature and heat transfer coefficient as compared to the rest of nanoparticle shapes..

References

- 1 Choi S U S, *ASME Publ Fed*, 231 (1995) 99.
- 2 Xuan Y & Li Q, *J Heat Transfer*, 125 (2003) 151.
- 3 Chein R & Chuang J, *Int J Therm Sci*, 46 (2007) 57.
- 4 Akbarinia A & Laur R, *Int J Heat Fluid Flow*, 30 (2009) 706.
- 5 Yang Y T & Lai F H, *Int J Heat Mass Transf*, 53 (2010) 5895.
- 6 Rana P & Bhargava R, *Commun Nonlinear Sci Numer Simul*, 16 (2011) 4318.
- 7 Hamad M A A & Ferdows M, *Commun Nonlinear Sci Numer Simul*, 17 (2012) 132.
- 8 Mital M, *Appl Therm Eng*, 52 (2013) 321.
- 9 Pal D & Mandal G, *Nucl Eng Des*, 273 (2014) 644.
- 10 Vanaki S M & Mohammed H A, *Int Commun Heat Mass Transf*, 67 (2015) 176.
- 11 Hayat T, Imtiaz M & Alsaedi A, *Adv Powder Technol*, 27 (2016) 1301.
- 12 Reddy P S & Chamkha A J, *J Porous Media*, 20 (2017) 1.
- 13 Khalid A, Khan I, Khan A, Shafie S & Tlili I, *Case Stud Therm Eng*, 12 (2018) 374.
- 14 Chaudhary S & Kanika K M, *S N Appl Sci*, 1 (2019) 1709.
- 15 Selimefendigil F & Öztop H F, *Int J Heat Mass Transf*, 129 (2019) 265.
- 16 Chaudhary S & Kanika K M, *J Porous Media*, 23 (2020) 27.
- 17 Chaudhary S & Kanika K M, *Phys Scr*, 95 (2020) 025202.
- 18 Mishra P, Acharya M R & Panda S, *Pramana*, 95 (2021) 52.
- 19 Allugavelli R, Balla C S, Naikoti K & Makinde O D, *Indian J Pure Appl Phys*, 60 (2022) 78.
- 20 Sakiadis B C, *AIChE J*, 7 (1961) 221.
- 21 Fang T, *Acta Mech*, 163 (2003) 161.
- 22 Mahmood M A A & Mahmoud M A E, *Acta Mech*, 181 (2006) 83.

- 23 Bachok N, Ishak A & Pop I, *Int J Therm Sci*, 49 (2010) 1663.
- 24 Mukhopadhyay S, Bhattacharyya K & Layek G C, *Int J Heat Mass Transf*, 54 (2011) 2751.
- 25 Chaudhary S & Kumar P, *Meccanica*, 49 (2014) 69.
- 26 Chaudhary S & Choudhary M K, *Eng Comput*, 35 (2018) 1675.
- 27 Anuar N S, Bachok N, Arifin N M & Rosali H, *Alex Eng J*, 59 (2020) 763.
- 28 Zainal N A, Nazar R, Naganthran K & Pop I, *Int J Numer Method H*, 31 (2021) 858.
- 29 Malvandi A, Hedayati F & Ganji D D, *Alex Eng J*, 52 (2013) 277.
- 30 Oztop H F & Abu-Nada E, *Int J Heat Fluid Flow*, 29 (2008) 1326.
- 31 Mohammad R & Kandasamy R, *J Mol Liq*, 237 (2017) 54.
- 32 Lin Y, Li B, Zheng L & Chen G, *Powder Technol*, 301 (2016) 379.
- 33 Yacob N A, Ishak A & Pop I, *Int J Therm Sci*, 50 (2011) 133.